

# Chugging Instability of H<sub>2</sub>O<sub>2</sub> Monopropellant Thrusters with Reactor Aspect Ratio and Pressures

Sungyong An\*

Korea Institute of Nuclear Safety, Daejeon 305-338, Republic of Korea

Jungkun Jin†

Samsung Heavy Industries Company, Ltd., Geoje 656-710, Republic of Korea  
and

Jeongsub Lee,‡ Sungkwon Jo,§ Daejong Park,¶ and Sejin Kwon\*\*

Korea Advanced Institute of Science and Technology, Daejeon 305-701, Republic of Korea

DOI: 10.2514/1.48939

Among the three types of instabilities, the low-frequency instability (chugging instability) was experimentally investigated with respect to the chamber pressure and aspect ratio ( $L/D$ ) of catalytic reactors in a monopropellant thruster. Three H<sub>2</sub>O<sub>2</sub> thrusters were used, and two parameters were found to be the dominant factors that generated a chugging instability of the order of several tens of hertz. A high chamber pressure and low  $L/D$  values (low pressure drop across the catalyst bed) were preferable for reducing pressure oscillation inside the reaction chamber. In addition, it was found that these two parameters were not independent but coupled; therefore, the point where chugging instability occurred varied slightly depending on the interaction between these parameters.

## Nomenclature

$A$	= cross-sectional area
$a$	= speed of sound, m/s
$C_d$	= discharge coefficient
$C^*$	= characteristic velocity, m/s
$D$	= diameter of reactor, mm
$G$	= mass flux, g/(s · cm <sup>2</sup> )
$L$	= length of reactor, mm
$\dot{m}$	= propellant mass flow rate, g/s
$P_1$	= feed pressure of propellant (upstream of injector), bar
$P_2$	= pressure upstream of catalyst bed (downstream of injector), bar
$P_3$	= reaction chamber pressure ( $P_c$ , downstream of catalyst bed), bar
$T_{ad}$	= adiabatic decomposition temperature, K
$\Delta P_{cat}$	= pressure drop across catalyst bed ( $P_2 - P_3$ ), bar
$\Delta P_{inj}$	= pressure drop across injector ( $P_1 - P_2$ ), bar
$\eta_{C^*}$	= efficiency of characteristic velocity, %
$\rho$	= density, kg/m <sup>3</sup>

## I. Introduction

ROCKET-GRADE hydrogen peroxide (RGHP) has been used as a monopropellant and storable oxidizer since the dawn of the space age. However, the demand for a higher specific impulse has

gradually led to the replacement of H<sub>2</sub>O<sub>2</sub> with another monopropellant: hydrazine. Furthermore, dinitrogen tetroxide has replaced H<sub>2</sub>O<sub>2</sub> for use as a storable oxidizer. Nevertheless, recent concerns about propellant toxicity have led to a renewed interest in H<sub>2</sub>O<sub>2</sub> for use in diverse propulsion systems for launch vehicles and satellites, despite the existence of alternative propellants exhibiting better performance [1]. Additionally, it has been possible for small-scale university laboratories, such as Purdue, Pisa, Surrey, and Tokyo Universities and Korea Advanced Institute of Science and Technology, to develop a thruster that uses this nontoxic propellant.

This interest has become apparent from recent papers on H<sub>2</sub>O<sub>2</sub>. The literature shows that recent research has been divided between two areas. The research in the first area has focused on the catalyst itself. In this research, catalyst characterizations, catalytic activity, and support effects have been investigated [2–9]. This research has been more extensive and specific than the research in the other area. The research in the second area involves the applications of H<sub>2</sub>O<sub>2</sub> decomposition, such as the design of various scale thrusters [10–14], propulsion modules for a satellite or lander [15–17], and a gas generator [18]. This research has focused on the performance evaluations of test thrusters (especially the decomposition efficiency for a continuous mode and the response characteristics for a pulse mode). However, activities related to the actual use, especially the pressure instability inside the reaction chamber, have not yet been undertaken. In a normal rocket, to achieve smooth combustion, the pressure oscillation inside the reaction chamber at a steady state should not exceed approximately  $\pm 5\%$  of the mean chamber pressure. Although a few analytical studies on the low-frequency instability of monopropellant thrusters have been conducted, considering their actual importance [19,20], just a few experimental or research results are available that analyze the pressure instability of H<sub>2</sub>O<sub>2</sub> monopropellant thrusters [21].

In the present study, the pressure roughness at a steady state was the primary focus because it directly affects the thruster force or impulse. Therefore, among the three types of instabilities [i.e., chugging (low frequency), buzzing (intermediate frequency), and screaming (high frequency)], the low-frequency, or chugging, instability was considered. This type of instability can be caused by resonances in the engine feed system or the coupling of structural and feed system frequencies [22]. In particular, the chugging instability has mainly appeared in low-thrust rocket engines designed with low-chamber-pressure engines (100–500 psia) [22], such as thrusters, which is in good accordance with the H<sub>2</sub>O<sub>2</sub> monopropellant thrusters

Received 19 January 2010; revision received 7 September 2010; accepted for publication 11 September 2010. Copyright © 2010 by the American Institute of Aeronautics and Astronautics, Inc. All rights reserved. Copies of this paper may be made for personal or internal use, on condition that the copier pay the \$10.00 per-copy fee to the Copyright Clearance Center, Inc., 222 Rosewood Drive, Danvers, MA 01923; include the code 0748-4658/11 and \$10.00 in correspondence with the CCC.

\*Senior Researcher, 34, Gwahak-ro, Yuseong-gu; k975asy@kins.re.kr.

†Senior Engineer, Marine Research Institute, 530, Jangpyung-ri, Sinhyeon-up; jungkun.jin@samsung.com.

‡Research Assistant, Division of Aerospace, 335, Gwahak-ro, Yuseong-gu; Qoo@kaist.ac.kr.

§Research Assistant, Division of Aerospace, 335, Gwahak-ro, Yuseong-gu; earthcsk@kaist.ac.kr.

¶Research Assistant, Division of Aerospace, 335, Gwahak-ro, Yuseong-gu; nasaboy@kaist.ac.kr.

\*\*Professor, Division of Aerospace, 335, Gwahak-ro, Yuseong-gu; trumpet@kaist.ac.kr. Member AIAA (Corresponding Author).

(below several hundred newtons) presently being tested by various research groups. For this reason, it is necessary to perform experimental tests to investigate the chugging instability in H<sub>2</sub>O<sub>2</sub> monopropellant thrusters. Therefore, reaction tests were performed with 50 N H<sub>2</sub>O<sub>2</sub> monopropellant test thrusters with different aspect ratios under different operating pressure conditions.

## II. Preparation for Experiments

### A. Catalyst and Propellant

MnO<sub>2</sub> was selected as the active material for H<sub>2</sub>O<sub>2</sub> decomposition because of its superior activity [5]. Commercial  $\gamma$ -type alumina pellets were crushed into grains with a mesh size of 16–20 (0.85–1.13 mm) to increase the effectiveness of the catalyst grains. The crushed grains were pretreated and loaded with NaMnO<sub>4</sub> by wet impregnation, using a precursor solution. The support was then dried (100°C, 24 h) and calcined (500°C, 2 h). The sodium ions were washed with water [9], and the catalyst-loaded grains were calcined (500°C, 2 h) again. Finally, MnO<sub>2</sub>/Al<sub>2</sub>O<sub>3</sub> (30 wt %) was prepared. The alumina pellets, crushed alumina grains, and prepared MnO<sub>2</sub>/Al<sub>2</sub>O<sub>3</sub> catalyst are shown in Fig. 1. The physical characteristics of the catalyst grains, such as specific surface area, pore volume, and average pore size (with ASAP 2420 analysis) were measured before and after catalyst coating. The crushed alumina grains had a specific surface area of 272 m<sup>2</sup>/g, a pore volume of 0.86 cm<sup>3</sup>/g, and an average pore size of 12.7 nm. After final calcination, the catalyst grain showed a slight decrease in specific surface area. Pore volume and average pore size changed to 0.61 cm<sup>3</sup>/g and 15.5 nm, respectively. Scanning electron microscope (SEM) images of MnO<sub>2</sub>/Al<sub>2</sub>O<sub>3</sub> are presented in Fig. 2.

Concentrated hydrogen peroxide (90 wt %) from peroxide propulsion was used as a monopropellant in the reaction test. The quality of propellant was nearly in accordance with the requirements of MIL-PRF-16005F [23], which defines the maximum allowable quantities of stabilizers and impurities for RGHP. The propellant density was 1392 kg/m<sup>3</sup> at room temperature. Theoretical adiabatic temperature  $T_{ad}$ , characteristic velocity  $C^*$ , and speed of sound  $a$  inside the reaction chamber obtained from the CEA (chemical equilibrium with applications) code calculations [24] were 1022 K (749°C), 936 m/s, and 697 m/s, respectively.

### B. Test Thrusters

The cross-sectional view of each thruster is shown in Fig. 3. Each thruster consists of the propellant inlet, inlet manifold, injector, catalytic reactor, distributor plate, and nozzle. To investigate the pressure-drop effect across the catalyst bed ( $P_2 - P_3$ ) with the chugging characteristics, three test thruster models were designed to have the same catalytic reactor volume (reaction ability) of  $14.1 \pm 0.1$  cm<sup>3</sup> but different reactor aspect ratios ( $L/D$ ), such as 0.50, 1.02, and 1.95. The inlet manifold (upstream injector) of all the thrusters was designed to have an identical volume. Because the injectors for all of the thrusters had identical  $C_d$  and  $A$  values in Eq. (1), the propellant had the same flow rate at a given pressure drop ( $\Delta P_{inj}$ ,  $P_1 - P_2$ ) across any given injector. Each injector had 15 orifices with diameters of 400  $\mu$ m. Catalyst grains would not escape from the reactor and would be located at their original position during the reaction tests. Therefore, a distributor plate was inserted downstream

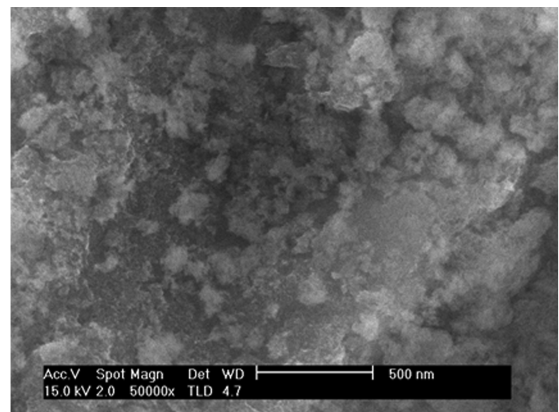
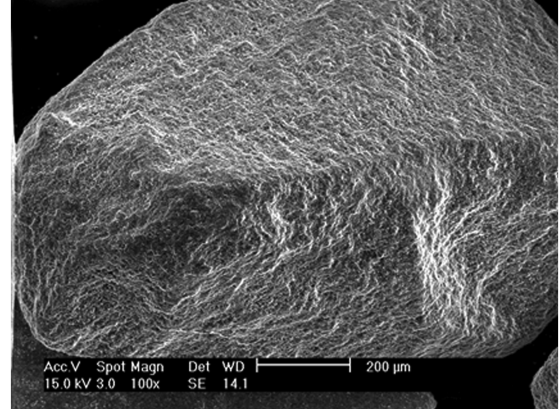


**Fig. 2 SEM images of MnO<sub>2</sub>/Al<sub>2</sub>O<sub>3</sub> catalyst grains. WD denotes work distance, SE denotes secondary electron, and TLD denotes through-the-lens deflector.**

of the catalyst bed. Its role was to support the catalyst grains. A screen having a small mesh size (less than catalyst grain size) was welded to the distributor structure. Figure 4 shows the shape of the injector and distributor with a welded screen. The chamber between the distributor and the nozzle throat was also designed to have the same volume as each thruster. Each thruster used a conical nozzle with a throat diameter of 4.9 mm and an area ratio of 2.6, which was the optimal expansion condition at a chamber pressure of 15 bar in a test performed at sea level. Figure 5 shows the position of each pressure port.  $P_1$ ,  $P_2$ , and  $P_3$  measured the propellant feed pressure (upstream of the injector), the pressure downstream of the injector (upstream of the catalyst bed), and the chamber pressure (downstream of the catalyst bed), respectively. Thus, the difference between  $P_1$  and  $P_2$  indicates the pressure drop across the injector  $\Delta P_{inj}$ , and the difference between  $P_2$  and  $P_3$  indicates the pressure drop across the catalyst bed  $\Delta P_{cat}$ . To measure the chugging instability, the pressure inside the reaction chamber  $P_3$  was considered:

$$\dot{m} = C_d A \sqrt{2\rho(P_1 - P_2)} \quad (1)$$



**Fig. 1 Alumina pellet, crushed alumina grains, and prepared MnO<sub>2</sub>/Al<sub>2</sub>O<sub>3</sub> catalyst.**

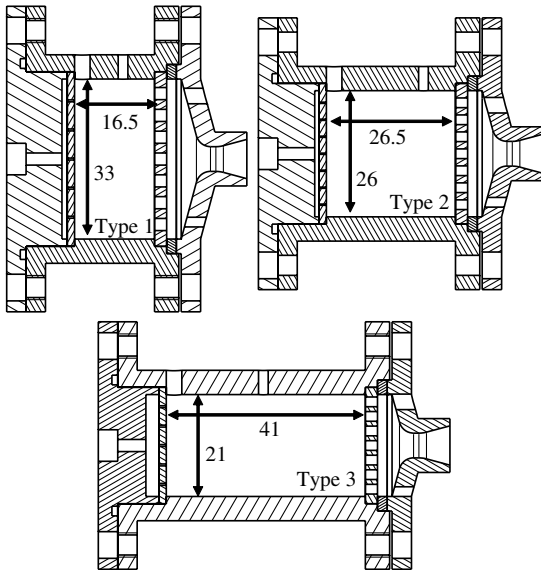


Fig. 3 Cross-sectional views of test thrusters (mm).

### C. Data Acquisition and Test Procedure

A schematic of the experimental thruster setup is shown in Fig. 6, which consists of a pressurizer gas tank, a hydrogen peroxide tank, pressure regulators, several control valves, a mass flowmeter, and valve control systems. A Coriolis-type mass flowmeter (AW Company, ACM600) with  $\pm 0.5\%$  precision was introduced to measure the propellant flow rate.

A data acquisition card and a signal conditioning extension for instrumentation modules with a 10 kHz filter from National Instruments were used to measure the physical data. The sampling rate during the tests was 500 samples/s, which was sufficient to detect several tens of hertz of chugging instability. During the tests, the product gas temperature at each position (1, 2, 3, ..., cm from catalyst upstream), the pressure ( $P_1$ ,  $P_2$ , and  $P_3$ ), and the propellant mass flow rate were measured.  $K$ -type thermocouples having an open junction were used to measure the temperature of product gases. The pressure sensors selected had 1 kHz dynamic characteristics.

The thrusters were filled with the prepared catalysts. Each test was performed using a pulse mode with a 1.0 s valve-on time and a 1.0 s

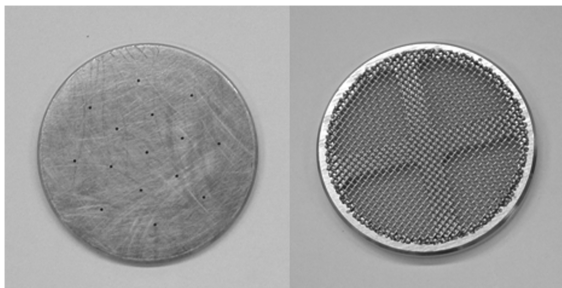


Fig. 4 Injector and distributor plate with welded screen.

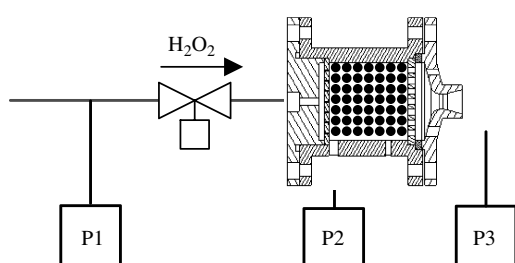


Fig. 5 Positions of pressure ports.

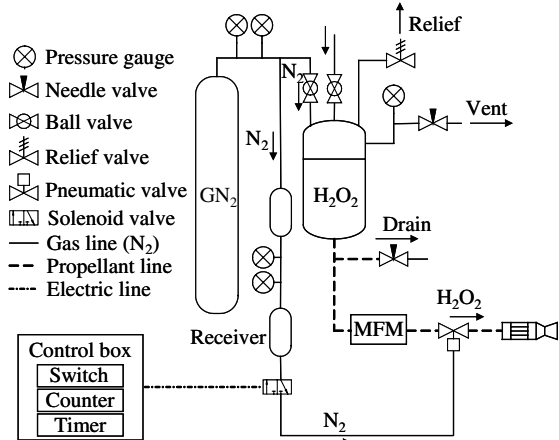


Fig. 6 Schematic of experimental test stand. MFM denotes mass flowmeter.

valve-off time to obtain repeated chugging instability results. During all the tests, the reactor was filled with an unused catalyst to eliminate any possibility of the catalyst bed characteristics (such as sintering, decrease in reactivity, grain crushing, and so on) affecting the chugging instability. In addition, the propellant feed pressure was set to values of around 10, 20, 30, and 40 bar to investigate the effect of pressure on the chugging instability.

### III. Results and Discussions

All the graphs for the reaction tests with the three thrusters are shown in Fig. 7. The pressures ( $P_1$ ,  $P_2$ , and  $P_3$ ) were measured to determine not only the pressure drops across the injector and the catalyst bed but also the chugging instability. Table 1 summarizes the pressure fluctuation from the mean chamber pressure at a steady state and its frequency.

First, chugging instabilities that exceeded  $\pm 5\%$  of the mean chamber pressure appeared in the lower left section of Fig. 7 (low feed pressure and high  $L/D$  condition), while there were no chugging phenomena in the cases shown in the upper right section (high feed pressure and low  $L/D$  condition), where the pressure oscillations were less than  $\pm 5\%$  of the mean chamber pressure. The frequency of the instability was several tens of hertz. A lower feed pressure ( $P_1$ ) resulted in a lower built pressure inside the reaction chamber ( $P_3$ ). The chugging phenomenon occurred dominantly when the chamber was at lower pressure. Therefore, the chamber pressure was the primary parameter while considering the instability criteria.

Although the chamber pressure was low, there was no chugging instability when  $L/D$  was low. For example, there was no chugging in the case of an  $L/D$  of 0.5 when  $P_1$  was 10 bar, but the instability did occur in the other two cases where  $P_1$  was 10 bar. The strength of the instability also increased when  $L/D$  increased. The  $L/D$  values of the reactors determined the pressure drop across the catalyst bed ( $\Delta P_{cat}$ ,  $P_2 - P_3$ ), which only occurs in the case of monopropellant thrusters. Therefore, the difference between  $P_2$  and  $P_3$  was directly related to the chugging instability. When the drop in pressure was low, there was no instability, even when  $P_3$  was very low. In addition, there was an instability tendency when the pressure drop across the catalyst bed ( $\Delta P_{cat}$ ,  $P_2 - P_3$ ) exceeded that across the injector ( $\Delta P_{inj}$ ,  $P_1 - P_2$ ).

From these results, to avoid the chugging instability, it was preferable to have: 1) a higher chamber pressure (higher feed pressure condition) and 2) a lower pressure drop across the catalyst bed. To reduce the pressure drop across the catalyst bed, it was beneficial for the reactor to have a low aspect ratio. In addition, it was also beneficial for the reactor to have a large catalyst grain. However, to use the large gain, the catalyst activity must be higher than the previous one if a given catalyst volume is used, because the reaction is restricted by the heat/mass diffusion phenomena in a large catalyst grain.

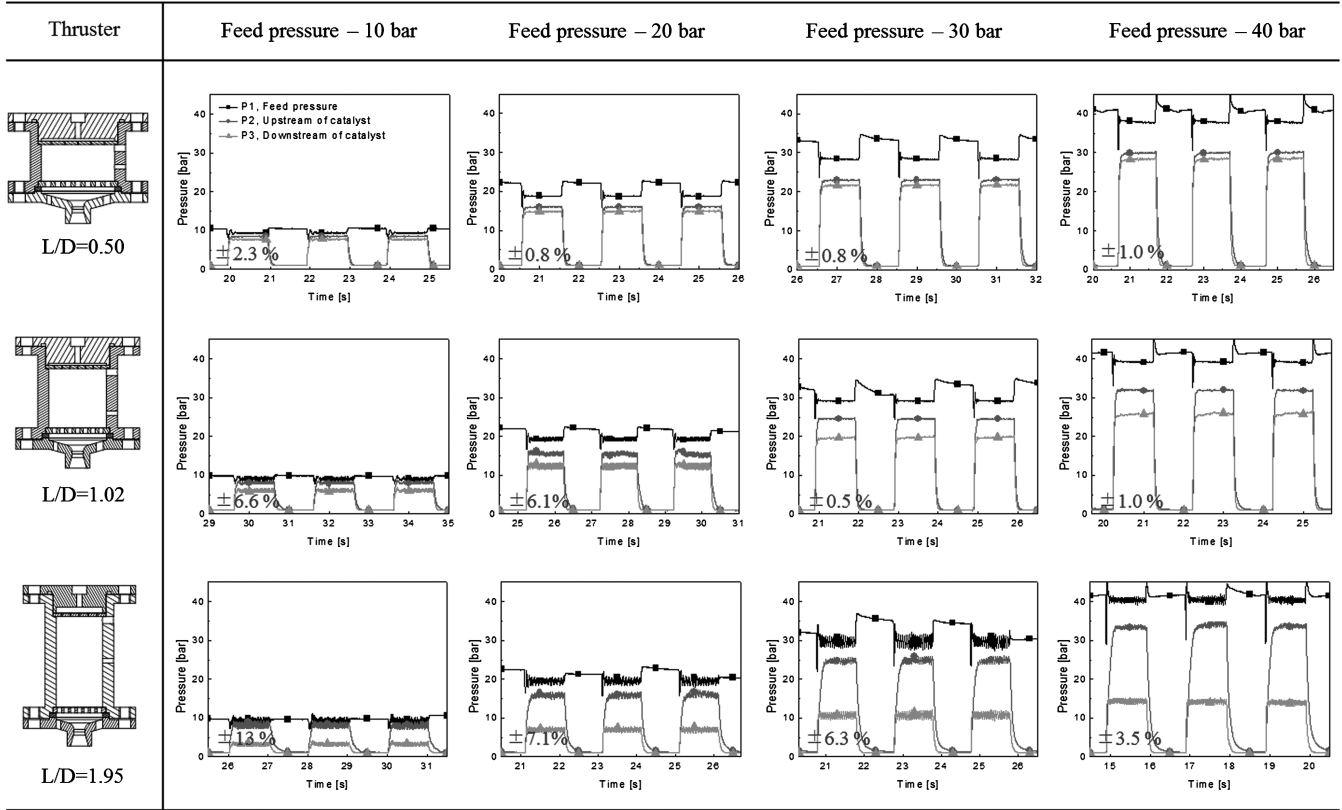


**Fig. 7** Pressure time histories for thrusters with different reactor  $L/D$  values and feed pressures.

Summerfield [19] used an analytical approach to determine the chugging instability tendency of monopropellant thrusters. He focused on the pressure drop across the injector, but he did not separate  $P_2$  and  $P_3$ . Instead of the  $(P_1 - P_2)$  value, the  $(P_1 - P_3)$  value was defined as the pressure drop across the injector. Thus, he could not observe the effect of the catalyst bed on the chugging instability, even though this effect should be a primary consideration for monopropellant thrusters. He also indicated that an increase in the pressure difference between the supply tank and combustion chamber could overcome the instability. To supplement this description, in the present study, the  $(P_2 - P_3)$  drop was found to be one of the main parameters that affected the chugging instability. As a result, although  $(P_1 - P_3)$  increased, the instability did not reduce in the experimental study when the pressure-drop increase was across the catalyst bed rather than across the injector.

Pressures ( $P_1$ ,  $P_2$ , and  $P_3$ ) and the instantaneously calculated propellant flow rates, with and without chugging instability (cases 1-1 and 3-1), are shown in Figs. 8 and 9, respectively. Instantaneous mass flow rates were calculated from the pressure drop across the injector, which determined the mass flow rates dominantly after the

pressure and temperature data reached a steady-state condition. There was no unsteady mass storage going on. The volume of the propellant tank (22 liter) was high enough compared with the test flow rates ( $9.4 \sim 67.1 \text{ g/s}$ ). When chugging instability occurred inside the reaction chamber ( $P_3$ ), it affected the upstream pressure ( $P_1$  and  $P_2$ ), which also resulted in the oscillation of the propellant flow rate. In addition, in most cases where the chugging instability was observed, the oscillation of feed pressure ( $P_1$ ) was 1.1–2.5 times higher in magnitude than that of the chamber pressure ( $P_3$ ). Phase differences among  $P_1$ ,  $P_2$ , and  $P_3$  were also observed. Figure 9 is a representative example and shows no phase difference among pressures. In all test cases,  $P_1$ ,  $P_2$ , and  $P_3$  were all in the same phase, which meant there was no traveling wave.

Johnson et al. [21] have analyzed the catalyst bed instability in the  $\text{H}_2\text{O}_2/\text{JP}-8$  bipropellant engine by separating the liquid and gas regions of the catalyst bed. However, although Johnson's paper could serve as a guideline for the chugging instability of  $\text{H}_2\text{O}_2$  monopropellant thrusters, it is incorrect to make a direct comparison because of the following reasons. First, in this research, some pressure drop occurs across the injector because of smaller diameter

**Table 1** Pressure oscillation of mean chamber pressure  $P_3$  and frequency in each reaction test

Case	Thruster ( $L/D$ )	$P_1$ , bar	$P_2$ , bar	$P_3$ , bar	$\Delta P_{\text{inj}}$ , bar	$\Delta P_{\text{cat}}$ , bar	$\dot{m}$ , g/s	$G$ , g/(s · cm <sup>2</sup> )	$\eta_{C^*}$ , %	Chugging frequency <sup>a</sup> , Hz	Chugging amplitude <sup>a</sup> , %
1-1	Type 1 (0.50)	9.5	8.5	7.7	1	0.8	18.3	2.1	92	50	±2.3%
1-2		18.7	15.9	14.8	2.8	1.1	32.0	3.7	101	53	±0.8%
1-3		28.4	23.1	21.8	5.3	1.3	50.9	6.0	93	53	±0.8%
1-4		37.9	30.2	28.6	7.7	1.6	67.1	7.8	93	53	±1.0%
2-1	Type 2 (1.02)	9.7	8.2	6.0	1.5	2.2	15.6	2.9	84	33	±6.6%
2-2		20.3	16.8	13.0	3.5	3.8	30.1	5.7	94	51	±6.1%
2-3		28.9	24.4	19.7	4.5	4.7	44.6	8.4	96	60	±0.5%
2-4		39.0	31.8	26.0	7.2	5.8	62.9	11.9	90	28	±1.0%
3-1	Type 3 (1.95)	9.4	8.8	3.4	0.6	5.4	9.4	2.7	79	29	±13.0%
3-2		19.3	15.7	6.9	3.6	8.8	17.9	5.2	84	48	±7.1%
3-3		29.2	24.7	10.8	4.5	13.9	27.0	7.8	87	63	±6.3%
3-4		40.3	32.6	13.7	7.7	18.9	38.8	11.2	77	73	±3.5%

<sup>a</sup>Calculated by chamber pressure  $P_3$ .

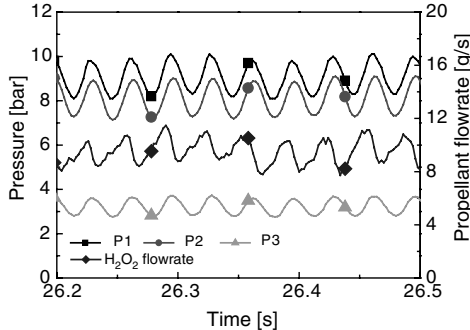


Fig. 8 Example of pressures and instantaneously calculated propellant mass flow rate with no chugging instability (case 1-1).

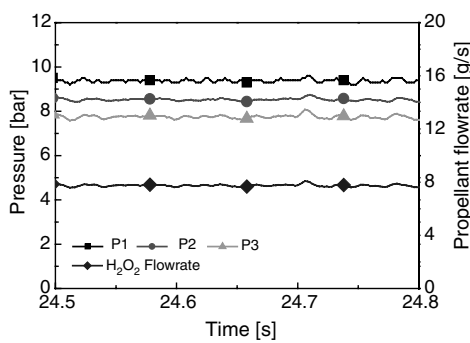


Fig. 9 Example of pressures and instantaneously calculated propellant mass flow rate with chugging instability (case 3-1).

orifices ( $400\ \mu\text{m}$ ). In [21], a distribution plate is present instead of an injector. There is a lower pressure drop ( $P_1 - P_2$ ) across a distribution plate than across an injector. The injector plays an important role in reducing the chugging instability, and an adequate pressure drop is necessary to control the chugging instability. Second, a grain-type catalyst was used for propellant decomposition in this study, whereas a screen-type silver catalyst was used in the previous reference. The difference in the type of catalyst used can affect chugging instability characteristics because of different flow pattern and decomposition phenomena.

The reduction of chugging instability by adding components, such as a cavitating venturi and gas accumulator to the propellant feeding line, was not considered, because the purpose of this study was to investigate the effect of the design of a monopropellant thruster itself on chugging instability. Moreover, these components cause additional pressure drop, which is considered a drawback in the design of a propulsion system.

For the most unstable test case (case 3-1; chugging amplitude:  $\pm 13.0\%$ ), the temperature profile of product gas as a function of pulse time is shown in Fig. 10. The temperature was measured at points located at 1, 2, and 3 cm on the catalyst bed (axial direction).

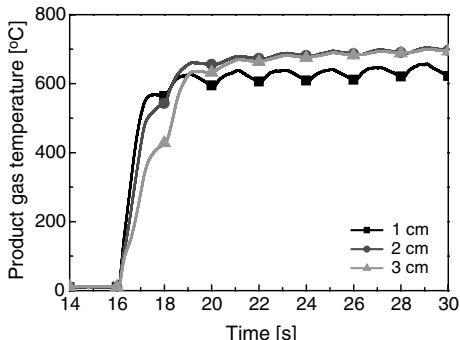


Fig. 10 Example of temperature profile with 1.0/1.0 s on/off pulse mode (case 3-1).

After two pulses, the temperature at each point reached the steady-state value, which was slightly below the theoretical adiabatic decomposition temperature. In this case, the speed of sound of the product gas was 680 m/s. A stable temperature was observed, contrary to the unstable pressure.

If the total flow area (open area) of the distributor plate (support structure placed after the catalyst bed) is small, the flow can be restricted, which would possibly affect the characteristics of the chugging instability. To avoid this problem, the distributor plate was designed to have a much higher flow area than that at the nozzle throat. The pressure drop across the distributor plate was negligible. Therefore, it was assumed that the total flow area of the distributor plate has no relationship with the nozzle throat area.

#### IV. Conclusions

Among the three types of instabilities in monopropellant thrusters, the low-frequency instability was experimentally investigated using H<sub>2</sub>O<sub>2</sub> monopropellant thrusters with respect to the chamber pressure and the aspect ratio of the reactors. Two parameters were found to be the dominant factors responsible for the chugging instability in H<sub>2</sub>O<sub>2</sub> monopropellant thrusters. A high chamber pressure and low  $L/D$  value (low pressure drop across the catalyst bed) were preferable for reducing the pressure oscillation inside the reaction chamber. In addition, these two parameters were not independent but coupled; therefore, the point where chugging instability occurred moved slightly, depending on the interaction between these parameters.

#### Acknowledgments

This work was supported by a grant from the Korea Science and Engineering Foundation provided by the Korean government (MEST) through National Research Laboratory (ROA-2007-000-20065-0).

#### References

- [1] Ventura, M., and Mullens, P., "The Use of Hydrogen Peroxide for Propulsion and Power," 35th AIAA/ASME/SAE/ASEE Joint Propulsion Conference and Exhibit, AIAA Paper 1999-2880, 1999.
- [2] Rusek, J. J., "New Decomposition Catalysts and Characterization Techniques for Rocket-Grade Hydrogen Peroxide," *Journal of Propulsion and Power*, Vol. 12, No. 3, 1996, pp. 574–579. doi:10.2514/3.24071
- [3] Tian, H., Zhang, T., Sun, X., Liang, D., and Lin, L., "Performance and Deactivation of Ir/ $\gamma$ -Al<sub>2</sub>O<sub>3</sub> Catalyst in the Hydrogen Peroxide Monopropellant Thruster," *Applied Catalysis A: General*, Vol. 210, Nos. 1–2, 2001, pp. 55–62. doi:10.1016/S0926-860X(00)00829-2
- [4] Pirault-Roy, L., Kappenstein, C., Guerin, M., and Eloirdi, R., "Hydrogen Peroxide Decomposition of Various Supported Catalysts Effect of Stabilizers," *Journal of Propulsion and Power*, Vol. 18, No. 6, 2002, pp. 1235–1241. doi:10.2514/2.6058
- [5] Kappenstein, C., Pirault-Roy, L., Guerin, M., Wahdan, T., Ali, A. A., Al-Sagheer, F. A., and Zaki, M. I., "Monopropellant Decomposition Catalysts. V. Thermal Decomposition and Reduction of Permanganates as Models for the Preparation of Supported MnO<sub>x</sub> Catalysts," *Applied Catalysis A: General*, Vol. 234, Nos. 1–2, 2002, pp. 145–153. doi:10.1016/S0926-860X(02)00220-X
- [6] Sorge, A. R., Turco, M., Pilone, G., and Bagnasco, G., "Decomposition of Hydrogen Peroxide on MnO<sub>2</sub>/TiO<sub>2</sub> Catalysts," *Journal of Propulsion and Power*, Vol. 20, No. 6, 2004, pp. 1069–1075. doi:10.2514/1.2490
- [7] Lim, H., An, S., Kwon, S., and Rang, S., "Hydrogen Peroxide Gas Generator with Dual Catalytic Bed for Non-Preheating Start-Up," *Journal of Propulsion and Power*, Vol. 23, No. 5, 2007, pp. 1147–1150. doi:10.2514/1.28897
- [8] Torre, L., Pasini, A., Romeo, L., Cervone, A., and D'Agostino, L., "Performance of a Monopropellant Thruster Prototype Using Advanced Hydrogen Peroxide Catalytic Beds," *Journal of Propulsion and Power*, Vol. 25, No. 6, 2009, pp. 1291–1299. doi:10.2514/1.44354
- [9] An, S., Lee, J., Brahmi, R., Kappenstein, C., and Kwon, S., "Comparison of Catalyst Support between Monolith and Pellet in

- Hydrogen Peroxide Thrusters," *Journal of Propulsion and Power*, Vol. 26, No. 3, 2010, pp. 439–445.  
doi:10.2514/1.46075
- [10] Kuan, C. K., Chen, G. B., and Chao, Y. C., "Development and Ground Tests of a 100-Millinewton Hydrogen Peroxide Monopropellant Microthruster," *Journal of Propulsion and Power*, Vol. 23, No. 6, 2007, pp. 1313–1320.  
doi:10.2514/1.30440
- [11] Pasini, A., Torre, L., Romeo, L., Cervone, A., and D'Agostino, L., "Testing and Characterization of a Hydrogen Peroxide Monopropellant Thruster," *Journal of Propulsion and Power*, Vol. 24, No. 3, 2008, pp. 507–515.  
doi:10.2514/1.33121
- [12] An, S., and Kwon, S., "Scaling and Evaluation of Pt/Al<sub>2</sub>O<sub>3</sub> Catalytic Reactor for Hydrogen Peroxide Monopropellant Thruster," *Journal of Propulsion and Power*, Vol. 25, No. 5, 2009, pp. 1041–1045.  
doi:10.2514/1.40822
- [13] An, S., Brahmi, R., Kappenstein, C., and Kwon, S., "Transient Behavior of H<sub>2</sub>O<sub>2</sub> Thruster: Effect of Injector Type and Ullage Volume," *Journal of Propulsion and Power*, Vol. 25, No. 6, 2009, pp. 1357–1360.  
doi:10.2514/1.46731
- [14] Lee, S. L., and Lee, C. W., "Performance Characteristics of Silver Catalyst Bed for Hydrogen Peroxide," *Aerospace Science and Technology*, Vol. 13, No. 1, 2009, pp. 12–17.  
doi:10.1016/j.ast.2008.02.007
- [15] An, S., Lim, H., and Kwon, S., "Hydrogen Peroxide Thruster Module for Microsatellites with Platinum Supported by Alumina as Catalyst," 43rd AIAA/ASME/SAE/ASEE Joint Propulsion Conference and Exhibit, AIAA Paper 2007-5467, 2007.
- [16] An, S., Jo, S., Wee, J., Yoon, H., and Kwon, S., "Preliminary Flight Test of Hydrogen Peroxide Retro-Propulsion Module," *Acta Astronautica*, Vol. 67, Nos. 5–6, 2010, pp. 605–612.
- [17] Sugawara, Y., Sahara, H., Nakasuka, S., Greenland, S., Morimoto, T., Koyama, K., Kobayashi, C., Kikuchi, H., Okada, T., and Tanaka, H., "A Satellite for Demonstration of Panel Extension Satellite (PETSAT)," *Acta Astronautica*, Vol. 63, Nos. 1–4, 2008, pp. 228–237.  
doi:10.1016/j.actaastro.2007.12.016
- [18] Park, D., An, S., and Kwon, S., "Design of Hydrogen Peroxide Gas Generator for Power Generation and Introduction of Measurement Method by an Automobile Turbocharger," 45th AIAA/ASME/SAE/ASEE Joint Propulsion Conference and Exhibit, AIAA Paper 2009-4833, Denver, 2009.
- [19] Summerfield, M., "A Theory of Unstable Combustion in Liquid Propellant Rocket Systems," *Journal of the American Rocket Society*, Vol. 21, No. 5, 1951, pp. 108–114.
- [20] Owens, W. L., "A Combustion Stability Analysis for Catalytic Monopropellant Thrusters," *Journal of Spacecraft and Rockets*, Vol. 9, No. 3, 1972, pp. 148–152.  
doi:10.2514/3.61644
- [21] Johnson, C., Anderson, W., and Ross, R., "Catalyst Bed Instability within the USFE H<sub>2</sub>O<sub>2</sub>/JP-8 Rocket Engine," 36th AIAA/ASME/SAE/ASEE Joint Propulsion Conference, AIAA Paper 2000-3301, 2000.
- [22] Sutton, G. P., *Rocket Propulsion Element*, 7th ed., Wiley-Interscience, New York, 2001.
- [23] "Performance Specification Propellant, Hydrogen Peroxide," U. S. Dept. of Defense, MIL-PRF-16005F, 1 Aug. 2003.
- [24] Stanford, G., and McBride, B. J., "Computer Program for Calculation of Complex Chemical Equilibrium Compositions and Applications," NASA, Publ. 1311, 1994.

D. Talley  
*Editor-in-Chief*